

COMPARISON OF WIND TUNNEL AND FULL-SCALE AERODYNAMIC SAIL FORCE MEASUREMENTS

Heikki Hansen¹, hhei005@ec.auckland.ac.nz
Peter Jackson², p.jackson@auckland.ac.nz
Karsten Hochkirch³, karsten.hochkirch@tu-berlin.de

Abstract. In this paper the comparison of aerodynamic sail force measurements from model scale wind tunnel and full-scale tests is presented. Wind tunnel testing of yacht sails is an effective design tool, but is at present mainly used for comparative testing. Comparing wind tunnel to full-scale data is important to better understand the associated scaling effects and make wind tunnel testing more accurate for quantitative sail force prediction. The full-scale data is taken from the sailing yacht DYNA developed at the Technical University of Berlin in Germany and is based on a 10-meter International Measurement System (IMS) cruiser/racer. For this project a 15% scale model was developed and upwind and downwind sail configurations comprising mainsail, genoa III and spinnaker were tested in the Twisted Flow Wind Tunnel (TFWT) of the University of Auckland. The parasitic drag was measured in the wind tunnel and compared to approximations used in velocity prediction programs (VPPs). The influence of the sails on the flow above the mast where the anemometer is located was investigated in the wind tunnel and the full-scale results are corrected to take this effect into account. The curves of lift and drag coefficient against the effective wind angle are compared to the coefficients obtained from the full-scale measurements. For the upwind configuration a significant force component up the mast was observed and its influence as the yacht heels was assessed. Comparing the results highlights the difficulties associated with modelling sail forces but also shows that wind tunnel and full-scale measurements complement each other.

NOMENCLATURE

β_A, β_{eff}	Apparent and effective wind angle
δ	Inclination angle of flow from xy-plane in body fixed coordinates
ϕ	Heel angle
AR, AS	Aspect ratio and reference sail area
C_D	Drag coefficient in body fixed coordinates
C_{Di}	Induced drag coefficient in body fixed coordinates
C_{DPA}	Parasitic drag coefficient in wind tunnel coordinates
C_{DPhull}	Parasitic drag coefficient of hull in wind tunnel coordinates
C_{Dspars}	Parasitic drag coefficient of spars in wind tunnel coordinates
C_{Dvis}	Viscous drag coefficient in body fixed coordinates
C_{FX}	Drive force coefficient in body fixed coordinates
C_{FY}	Side force coefficient in body fixed coordinates
C_{FZ}	Coefficient of force up the mast in body fixed coordinates
C_{FZA}	Vertical force coefficient in wind tunnel coordinates
C_{FYP}	Parasitic side force coefficient in body fixed coordinates
C_L	Lift coefficient in body fixed coordinates
C_{LA}	Lift coefficient in wind tunnel coordinates
e	Efficiency factor
q_A, q_{eff}	Apparent and effective dynamic pressure
V_A, V_{eff}	Apparent and effective wind velocity
x, y, z	Coordinates in body fixed system

1. INTRODUCTION

Velocity Prediction Programs (VPPs) predict the performance of a sailing yacht by balancing the aerodynamic and hydrodynamic forces and moments so that the vessel sails in equilibrium. The aerodynamic and hydrodynamic force and moment coefficients used by a VPP are determined in a number of ways using theoretical models, computational fluid dynamics (CFD) or experimental methods. Obtaining coefficients from full size tests is desirable but too complicated and expensive and so has only been attempted in a few research projects. The aerodynamic sail force coefficients can be determined by conducting wind tunnel tests. The controllable environment of a wind tunnel has many advantages and is a much more cost effective solution. On the other hand little is known about the scaling effects associated with wind tunnel testing of yacht sails. It is hence important to compare full scale and wind tunnel measurements to assess these effects and validate results obtained through wind tunnel testing.

2. FULL-SCALE AERODYNAMIC DATA

In order to measure the aerodynamic and hydrodynamic forces and moments separately a specially constructed sail force dynamometer is required, due to the large pretension in the rig and the comparatively small resultant aerodynamic forces. Milgram first introduced this concept in 1988 as the MIT sailing dynamometer [1]. On this 35ft yacht all rigging components were connected to a framework structure inside the hull and deck shell. A six-component force balance measured the

¹ Graduate Student (PhD), Mechanical Engineering Department, University of Auckland, New Zealand

² Professor, Mechanical Engineering Department, University of Auckland, New Zealand

³ Dr.-Ing., Institut für Land- und Seeverkehr, Technische Universität Berlin, Germany

forces between the frame and the hull. Model rigs of a Maxi yacht and an International America's Cup Class (IACC) yacht were investigated. The results are compared with theoretical methods but to the authors' knowledge no wind tunnel testing was carried out. In 1997 a similar concept was used on the sailing dynamometer FUJIN [2] to obtain aerodynamic force coefficients of an IACC and International Measurement System (IMS) rig and validate numerical calculation methods.

The most recent project to determine the full-scale forces acting on a sailing yacht was initiated at the Technical University of Berlin in Germany in 1996 [3], in order to investigate the relation between model tests, numerical simulations and full size data. A 10-metre full-scale sail force dynamometer named DYNA (Figure 1) was designed and built. The hull and rig are based on a modern 33ft IMS cruiser/racer yacht to provide suitable reference results for contemporary yacht design issues. In addition to the force balance between the internal frame and hull, multi component force balances also measured the hydrodynamic loads on keel and rudder. This full-scale aerodynamic data is used here for the comparison to wind tunnel tests.



Figure 1. DYNA acquiring full-scale data

3. TWISTED FLOW WIND TUNNEL

The tests are conducted in the open circuit Twisted Flow Wind Tunnel (TFWT), which has been developed by the University of Auckland [4] especially for testing yacht sails. Sails experience a change in apparent wind velocity (V_A) and angle (β_A) with height above the water due to the speed of the yacht and the velocity gradient in the true wind. This sheared and twisted flow is simulated in the TFWT by generating flow with a planetary boundary layer velocity profile that is twisted by vertical vanes situated upstream of the test section (Figure 2), which is 7 meters wide and 3.5 meters high.

A six-component force balance is located under the wind tunnel floor in the test section. Three brackets of the balance protrude through the tunnel floor to hold the model. The force balance can be turned together with the floor above (turntable) to change the apparent wind angle, so that the forces are measured in a coordinate system aligned with the centreline of the model and the horizontal plane (coordinate system A). The turntable has a recess to allow the waterline of the hull to coincide with the wind tunnel floor. The recess is filled with water to prevent any flow under the hull.



Figure 2. Model with mainsail and spinnaker in the TFWT

4. WIND TUNNEL MODEL

A 15% scale model of DYNA was designed and built comprising of sails, rig, load carrying frame, deck and hull (Figure 2). A cradle connects the model to the force balance and allows adjusting of the heel angle (ϕ). The model can be rotated about a fixed axis on its centreline and 115mm above the design waterline to approximate the heeling behaviour of the yacht. The model can be

heeled to any angle but is not free to dynamically adjust its heel angle depending on the overturning moment. A similar concept to DYNA with a load carrying internal frame was chosen due to future research plans of decoupling the sail and hull forces (Figure 3). The model is fitted with six winches to trim the sails remotely.

4.1. Model sails

The model sails were built from the same geometrical descriptions as the full-scale sails. The desirable properties are also similar, lightness with minimal stretch but the elastic scaling is not accounted for. The mainsail and genoa III (100%) were built from 9933 polyester and the symmetrical spinnaker of Contender Superlite (polyester).



Figure 3. The load carrying internal frame of the model

5. VELOCITY AND TWIST PROFILES

Wind tunnel tests with the mainsail and genoa III were conducted at heel angles of 0° , 12.5° and 25° for apparent wind angles between 10° and 90° . For these apparent wind angles the expected twist in the onset flow over the span of the sails ranges from 2.2° to 8.5° . These tests were not conducted in twisted flow since the disadvantages of having the vanes in the flow exceed the advantages for these small twist angles. The wake behind the vanes introduces unevenly distributed turbulence in the flow. An approximate logarithmic vertical velocity profile in the onset flow was achieved by placing a trip board in the wind tunnel upstream of the test section. The velocity change over the span of the sails was about 20%. This profile was used for all tests conducted with the mainsail and genoa III. The reference flow velocity was about 3.7m/s.

Tests were also carried out with the mainsail and spinnaker at 0° heel angle for apparent wind angles between 45° and 180° . For the majority of apparent wind angles in this range the twist in the onset flow is similar. Hence only one twist profile was developed which twists the flow through 9.5° over the span of the sails. The

velocity change over the span of the sails was about 26% and the reference flow velocity approximately 2.6m/s.

The reference height for defining the apparent wind angle and velocity is taken as the geometric centre of sail area height. It is hence dependent on the heel angle.

6. FORCE COEFFICIENTS

In the wind tunnel the drive force (F_{XA}) and side force (F_{YA}) are measured in a horizontal plane, where the drive force is parallel to the centreline of the yacht and the side force perpendicular to it. The vertical force (F_{ZA}) is positive upwards. The full-scale measurements are taken in the body fixed coordinate system of the yacht (coordinate system B). The forces $\mathbf{F}_A=(F_{XA} F_{YA} F_{ZA})^T$ and moments $\mathbf{M}_A=(M_{XA} M_{YA} M_{ZA})^T$ measured in the wind tunnel in coordinate system A are transformed to coordinate system B by rotating through the heel angle with

$$\mathbf{T}_\phi = \begin{bmatrix} 1 & 0 & 0 \\ 0 & \cos\phi & \sin\phi \\ 0 & -\sin\phi & \cos\phi \end{bmatrix} \quad (1)$$

and translating through $\overline{\mathbf{AB}}$, the distance between the coordinate systems origins (measured in coordinate system A, to obtain $\mathbf{F}_B=(F_X F_Y F_Z)^T$ and $\mathbf{M}_B=(M_X M_Y M_Z)^T$ from

$$\overline{\mathbf{F}}_B = \mathbf{T}_\phi \overline{\mathbf{F}}_A, \quad (2)$$

$$\overline{\mathbf{M}}_B = \mathbf{T}_\phi \overline{\mathbf{M}}_A + \mathbf{T}_\phi (\overline{\mathbf{F}}_A \times \overline{\mathbf{AB}}). \quad (3)$$

F_Z in body fixed coordinates is here referred to as the force acting up the mast. In this description mast rake, bend and deflection are ignored and the mast is assumed to be aligned with the z-axis.

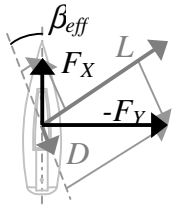
In the wind tunnel the apparent wind velocity and angle are measured in the horizontal plane. The effect of heeling can be incorporated in the apparent wind angle to form an effective angle (β_{eff}) if the sails are assumed to be insensitive to span wise flow [5]. The effective angle is then the apparent angle in a plane normal to the z-axis and given by

$$\beta_{eff} = \arctan(\tan \beta_A \cos \phi), \quad \beta_{eff} \in [0, 180^\circ]. \quad (4)$$

Similarly the effective velocity (V_{eff}) is defined as the component of incident flow in a plane normal to the z-axis and calculated from

$$V_{eff} = V_A \sqrt{1 - \sin^2 \beta_A \sin^2 \phi}. \quad (5)$$

Drag (D) is defined as the force in line with the onset flow and Lift (L) as being perpendicular to it. They can be obtained from F_X and F_Y by rotating the coordinate system through the effective wind angle with



$$\begin{pmatrix} L \\ D \end{pmatrix} = \begin{bmatrix} \sin \beta_{eff} & \cos \beta_{eff} \\ -\cos \beta_{eff} & \sin \beta_{eff} \end{bmatrix} \begin{pmatrix} F_X \\ -F_Y \end{pmatrix}. \quad (6)$$

It is convenient to write forces in non-dimensional coefficient form. The lift coefficient for example is given by

$$C_L = \frac{L}{0.5 \rho_{air} V_{eff}^2 AS} = \frac{L}{q_{eff} AS}, \quad (7)$$

where the rated reference sail area (AS) is determined from the mainsail area (AS_{main}) and the fore triangle with

$$AS = \frac{AS_{main}}{1.16} + \frac{IJ}{2}. \quad (8)$$

The total drag is the sum of the induced drag and the viscous drag. In coefficient form it can be written as

$$C_D = C_{Dvis} + C_{Di} = C_{Dvis} + \frac{C_L^2}{\pi e AR}. \quad (9)$$

The induced drag (C_{Di}) is ideally a function of the lift coefficient squared and depends on the aspect ratio (AR) and the efficiency (e). The viscous drag coefficient (C_{Dvis}) consists of the skin friction and separation drag, which cannot easily be separated.

7. FLOW ABOVE THE MAST

The wind direction and velocity for the full-scale tests are measured with a cup anemometer and direction vane situated 850mm above the top of the mast. Calibration tests on DYNA showed that the anemometer is insensitive to flow along its rotation axis in upwind sailing conditions with up to 30° of heel. Hence only the flow component in a plane normal to the rotation axis is measured. If the rotation axis is assumed to be parallel to z-axis the measured velocity and angle are equivalent to the effective velocity and angle calculated for the wind tunnel experiments.

The influence of the sails and rig on the free stream flow at the position of the cup anemometer was determined in the wind tunnel by measuring the change in flow direction and velocity at the corresponding height above the top of the mast. The experimental set-up and data acquisition software was developed based on previous work [6]. A five-hole, hemispherical head, pitot tube, which can measure flow angles of up to $\pm 30^\circ$ from its centre line, was suspended from the wind tunnel ceiling. A Setra 239 pressure transducer sequentially measured the pressures at the five pitot tube openings. A second pressure transducer measured a reference pressure to

account for any drift in the free stream flow. Due to the small pressures and the range of the pressure transducers available, the accuracy of the resultant dynamic pressure was $\pm 5\%$, while flow angles can be measured with an accuracy of $\pm 0.5^\circ$.

For all effective angles the effective angle was found to be increased by the presence of the sails (Figure 4). The increase is largest for small effective angles and reduces as the effective angle increases. The change in effective angle tends to increase with heel angle. A direct comparison to other work is difficult since many factors influence the effect. Wind tunnel tests of a 1/6 scale One Tonner model by Kamman [7] show an increase in effective angle of about 5° in a similar position above the mast, for tests at an effective angle of 25° and heel angle of 20° .

Due to the limited absolute accuracy of the pressure transducer the measured change in dynamic pressure is only indicative. The effective dynamic pressure seems to increase by 10 to 15% due to the sails when sailing upwind and reduce by 5 to 10% when going downwind (Figure 5). The full-scale measurements reported here have been corrected for this change in effective angle and velocity due to the sails.

The angle of the flow out of a plane normal to the z-axis is here called inclination angle (δ). The flow is directed up the mast and the change in inclination angle increases with effective and heel angles (Figure 6). Due to the heel angle the horizontal free stream flow has an angle relative to the xy-plane. A total inclination angle of more than 25° under mainsail and genoa III is unlikely since a heel angle of 25° cannot be expected at effective angles larger than 50° . With mainsail and spinnaker the change in inclination angle of the flow is about 15° at 0° heel. A yacht can heel up to 25° under spinnaker when reaching which increases the inclination angle significantly. In such a condition the calibration of a cup anemometer is likely to be effected. For other types of yachts with a masthead spinnaker and more roach on the mainsail the inclination angle could be significantly larger.

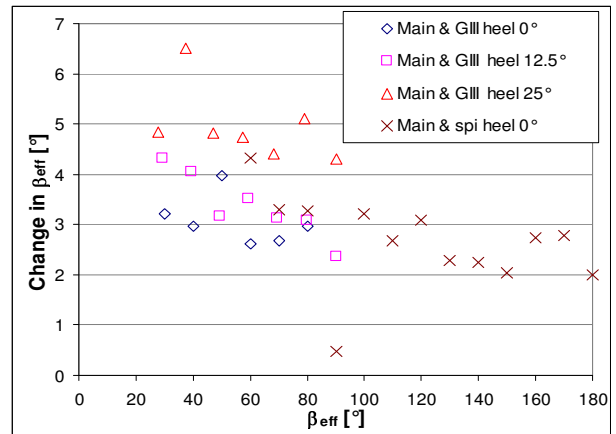


Figure 4. Change in effective angle (β_{eff}) of flow 130mm above mast due to presence of sails

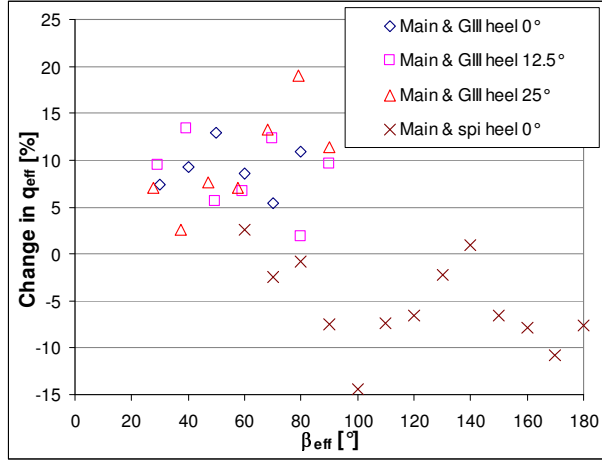


Figure 5. Change in q_{eff} of flow 130mm above mast due to presence of sails

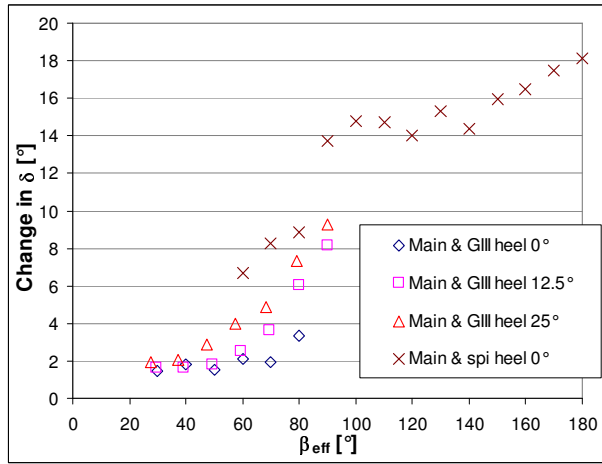


Figure 6. Change in inclination angle (δ) of flow 130mm above mast due to presence of sails

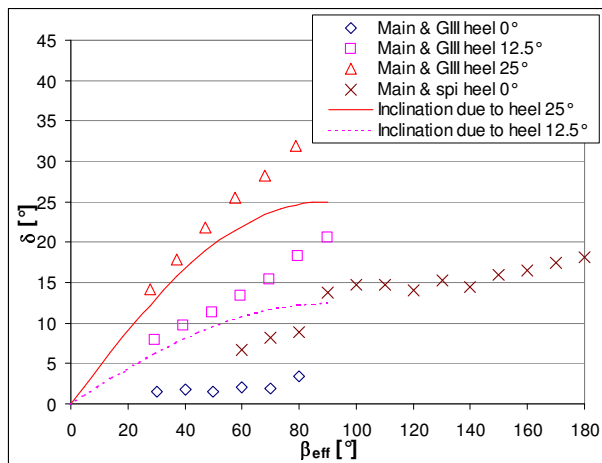


Figure 7. Inclination angle (δ) of flow 130mm above mast for mainsail with genoa III and with spinnaker

8. PARASITIC DRAG OF SPARS AND HULL

The parasitic drag of the spars and hull was determined by measuring the forces acting on the model without sails. Measurements were conducted for the upwind and downwind test configuration to ensure that the effect of different velocity and twist profiles was correctly accounted for. No clear trend of the horizontal parasitic drag coefficient (C_{DPA}) with heel angle was seen (Figure 8). The VPP developed as part of the DYNA project approximates the C_{DPA} in two parts [3]. The component of the spars is described by

$$C_{Dpspars} = \frac{C_{DPX} AP_X |\cos \beta_A| + C_{DPY} AP_Y |\sin \beta_A|}{AS} \quad (10)$$

With the sail area (AS) in the denominator the C_{DP} can be added directly to other drag coefficients. The area of the spars projected on the x-plane (AP_X) is multiplied by the parasitic drag coefficient in the x-direction (C_{DPX}) and the cosine of the apparent wind angle (β_A). Similarly the drag component from the area projected on the y-plane (AP_Y) is determined. C_{DPX} and C_{DPY} are taken from [8] as 0.8 and 1.13, respectively [3].

The parasitic air drag coefficient of the hull ($C_{DP_{hull}}$) is approximated by

$$C_{DP_{hull}} = k \frac{AP_{XH} |\cos \beta_{AH}| + AP_{YH} |\sin \beta_{AH}|}{AS} \quad (11)$$

where

$$k = c_0 f_{VA}^2 \quad (12)$$

$$\beta_{AH} = \sin(\beta_A + \tau) \quad (13)$$

AP_{XH} is the hull area above the waterline projected on the x-plane and AP_{YH} the area projected on the y-plane. The constant c_0 was determined from the full-scale measurements to be 0.764. The wind direction and velocity to calculate the parasitic hull drag coefficient were taken at the height of the hull, so that the apparent wind angle needs to be corrected by the flow angle change (τ) between the reference height and the height of the hull. The change in apparent wind velocity between the reference height and the height of the hull is accounted for by a velocity factor (f_{VA}).

The total horizontal parasitic drag measured in the wind tunnel is significantly less than predicted by the DYNA VPP (Figure 8). The correct velocity profile close to the floor of the wind tunnel is difficult to achieve and due to the large velocity gradient measuring f_{VA} accurately is problematical. Scaling effects caused by Reynolds Number changes and the level of detail modelled in the wind tunnel can also influence the parasitic drag components. The full-scale parasitic drag of the hull is estimated by system identification of the data acquired while sailing and therefore these reading take into account the interaction between hull/deck, spars and sails

while the wind tunnel data was measured without the sails set. The air resistance coefficient of the hull (c_D) determined from the full-scale tests is much smaller than the hydrodynamic coefficients and inaccuracies are hence likely. The parasitic drag of the spars has not yet been measured on DYNA.

However the shape of the modelled curves and the wind tunnel results is similar and approximating the parasitic drag with equations of this form (Equation 10 and 11) is feasible. Wind tunnel measurements of parasitic hull and spars drag by Campbell [9] indicated that the C_{DP} can alternatively be described by a sinus squared function and Figure 8 shows that this is also the case for the data presented here. Further tests are planned in the wind tunnel to investigate the hull and spars components separately. Not only the parasitic drag coefficient, but all six force and moment coefficients acting on the model without sails are subtracted from the results when testing with sails to give the sail force coefficients.

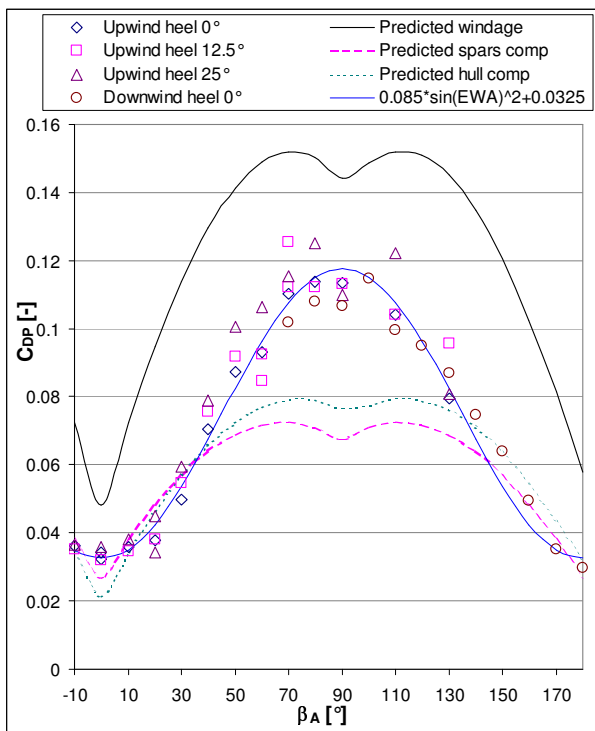


Figure 8. Parasitic drag coefficient of model in horizontal plane and predicted by the DYNA VPP

9. COMPARISON OF AERODYNAMIC FORCES

The full-scale results have a lot of scatter due to the constantly changing testing environment and the data fitting has a great influence on the resulting curves. The amount of scatter in the full-scale data is indicated on the graphs by a region above and below the modelled curve that includes 50% of the analysed data points. The standard deviation is calculated with respect to the values expected from the modelled curve. In most cases between 66% and 72% of the data points are within one

standard deviation. A fraction of one standard deviation is plotted on the graphs so that 50% of the data lie within the shown region.

In the wind tunnel it is possible to try a number of different sail trims to find the ‘optimal’ setting for each sailing condition. This is much more difficult in full-scale testing and care must be taken when analysing the data. In the wind tunnel the sails were trimmed to maximise the drive force coefficient (C_{FX}) in order to approximate the optimal lift coefficient for each test condition. In many real life sailing conditions it is necessary to reduce the overturning moment to avoid excessive heel angles by twisting off the mainsail. Reducing the overturning moment is however not considered here since it complicates the trimming process further and maximum lift coefficients are required as VPP input parameters.

9.1. Drive force coefficients

The drive force coefficient data from the wind tunnel tests show little scatter since C_{FX} is monitored when trimming the sails. The scatter in the full-scale data for mainsail and genoa III is small compared to the mainsail and spinnaker data (Figure 9). One standard deviation of the full-scale data is 0.058 and 0.304 respectively. Other force coefficients show a similar trend. When sailing downwind the flow partially separates along the cord of the sails. The separation point depends on the sail trim and dynamic effects like the yacht motion and changes in apparent wind angle. The distribution between the lift and drag components can vary significantly, which explains the larger amount of scatter in the down wind data. The wind tunnel and full-scale data sets show similar trends but the drive force is under predicted in the wind tunnel. While the agreement here is quite good, C_{FX} cannot be used directly in VPPs but is calculated from C_L and C_D .

9.2. Lift and drag coefficients

The lift and drag coefficients obtained from the full-scale data for mainsail and spinnaker show a similar amount of scatter with one standard deviation being 0.274 and 0.264 respectively. The scatter again is more than for the mainsail and genoa III combination. However the model C_L agrees well with the full-scale results (Figure 10). The C_D has a different trend; in the wind tunnel it is under predicted for effective angles larger than 130° and over predicted at smaller effective angles. Effective angles less than 80° are usually not achieved on DYNA when sailing with spinnaker and the full-scale results in this region are based on a small number of measurement points.

For mainsail and genoa III the viscous drag coefficient ($C_{D_{vis}}$) is plotted. The efficiency factor (e) obtained from the full-scale measurements as 1.1 [3] is used to calculate the induced drag coefficient. The $C_{D_{vis}}$ shows a similar

trend of being over predicted at small effective angles and under predicted at larger angles (Figure 11). Below effective wind angles of about 25° the full-scale C_{Dvis} is negative. The C_D however is not negative but the subtraction of C_{Di} is responsible for the change in sign. The lift coefficient for mainsail and genoa III is modelled from the full-scale measurements by manually fitting a curve through the highest data points to approximate the maximum C_L . The region in which 50% of the data points lie therefore only extends below this curve (Figure 12). The C_L is under predicted in the wind tunnel. Apart for small effective wind angles the results for the different heel angles do not collapse onto one curve as the simple theory anticipates. The lift coefficient reduces with increasing heel angle.

An alternative way to plot wind tunnel data for different heel angles is to calculate the lift coefficient in the horizontal plane (C_{LA}) and obtain the component in the heeled plane by dividing by the cosine of the heel angle [10]. This is only correct if no force acts along the mast as assumed in VPPs. The measurements for different heel angles more closely collapse onto one curve (Figure 13).

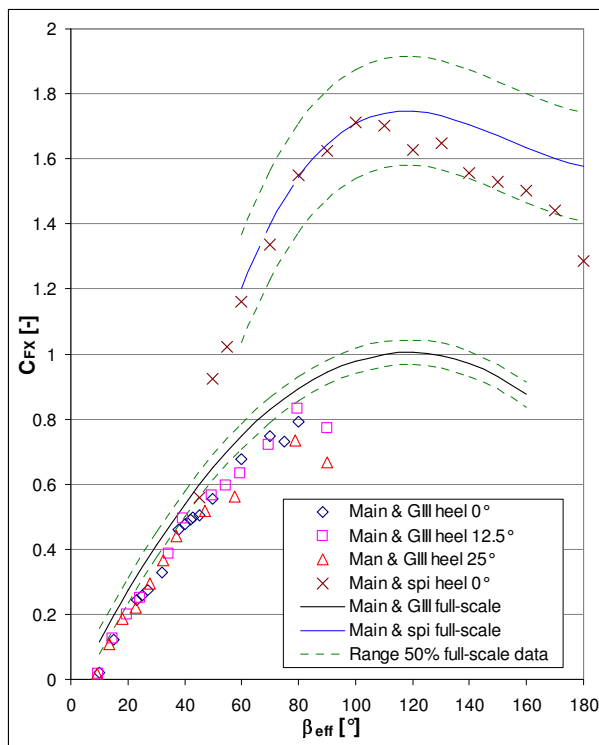


Figure 9. Drive force coefficient for mainsail with genoa III and with spinnaker

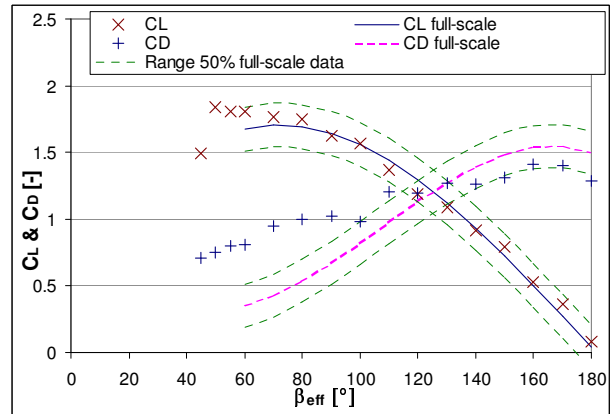


Figure 10. Lift and drag coefficients for mainsail and spinnaker

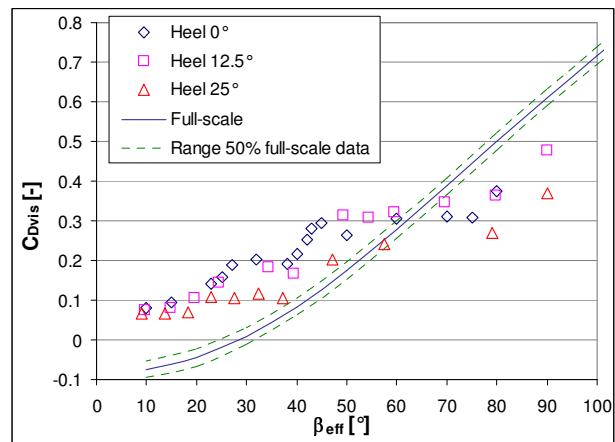


Figure 11. Viscous drag coefficient for mainsail and genoa III

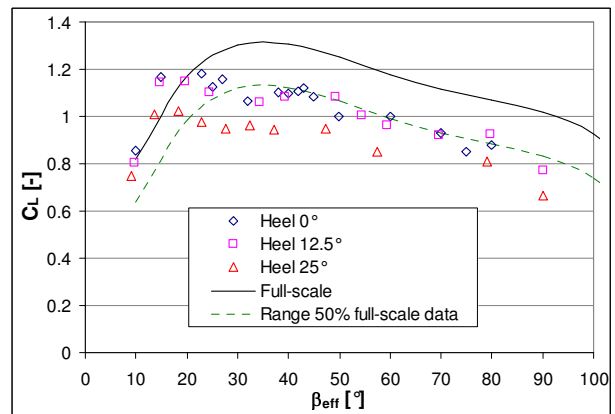


Figure 12. Lift coefficient for mainsail and genoa III

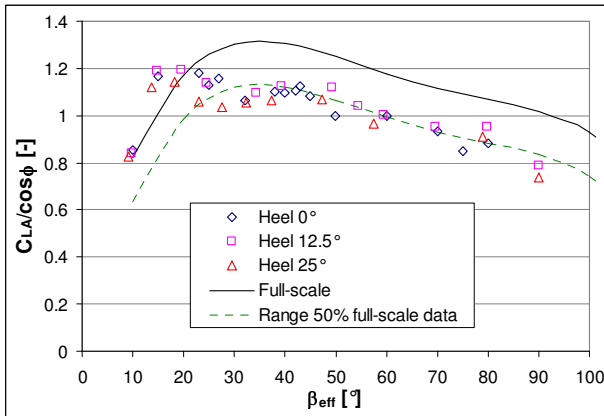


Figure 13. Horizontal lift coefficient divided by the cosine of the heel angle for mainsail and genoa III

9.3. Forces up the mast

Previous research in the TFWT [10] has shown the presence of a significant force component up the mast, of up to 10% of the side force. It is believed that the sails, hull and the interaction between the two contribute to it. From the wind tunnel tests on the DYNA model it was verified that a yacht without sails produces a force up the mast (Figure 14). The flow around the hull and deck is accelerated which causes a low-pressure region over the deck and a force up the mast. From the wind tunnel tests without sails it can be seen that this force tends to increase with heel angle.

As expected, wind tunnel tests with mainsail and genoa III show an additional force component up the mast (Figure 15). Which again increases with heel angle. In contrary C_{FZ} from the full-scale measurements is almost zero. On the sailing dynamometer the forces on the sails and rig are measured and corrected by the spars windage approximation (Equation 10) to give the sail forces. In the wind tunnel on the other hand the forces on the sails, rig and hull/deck are measured and corrected by the forces acting on the rig and hull/deck without the sails. Hence the wind tunnel sail forces include the interaction forces between the sails and hull/deck, which are not part of the full-scale forces. This indicates that the force up the mast results from the interaction between the sails and hull/deck and not from the sails themselves. The presence of the sails could accelerate the flow over the deck further which increases the force up the mast. Varying complex flow patterns can be expected over the deck for different effective angles. C_{FZ} however does not change much with the effective angle (Figure 15). Further wind tunnel tests are planned to investigate this interaction.

To the authors' knowledge the effect of the force up the mast is currently not accounted for in VPPs. Depending on the course sailed, the resultant vertical force is positive or negative (Figure 16). In 20 knots of true wind for example, the vertical force can increase the displacement of the vessel by up to 2.5% when going

upwind and realistically reduces it by up to 1.5% when sailing downwind. The influence on the hydrodynamic performance is relatively small.

The force up the mast has a more significant influence on the aerodynamic side force. In VPPs the aerodynamic lift and drag coefficients are defined in the heeled plane. For an effective angle F_X and F_Y in the heeled plane are calculated and F_Y multiplied by the cosine of the heel angle to obtain the horizontal side force. As the yacht heels a component of the force up the mast acts sideways which is not accounted for in the VPP force model. For a heel angle of 25° the horizontal side force increases by 10 to 15% when including the component of the force up the mast (Figure 17).

Figure 12 and Figure 13 show that the effect of heeling is better accounted for when plotting $C_{Lhor}/\cos\theta$. This method is however not based on sound aerodynamic principles in this situation since a force is acting up the mast. The effective angle theory does not account for all the heeling effect since the lift coefficient reduces with heel angle (Figure 12).

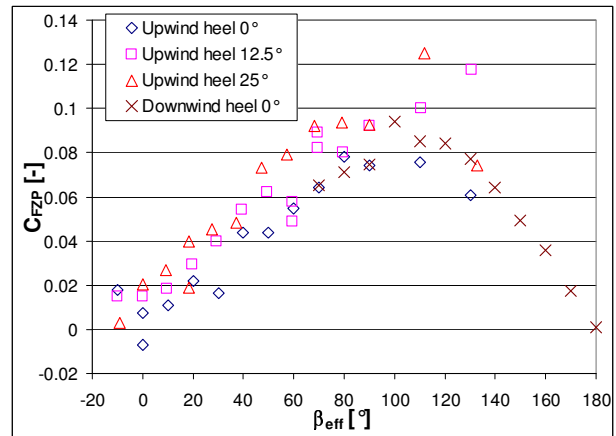


Figure 14. Coefficient of force up the mast for model without sails

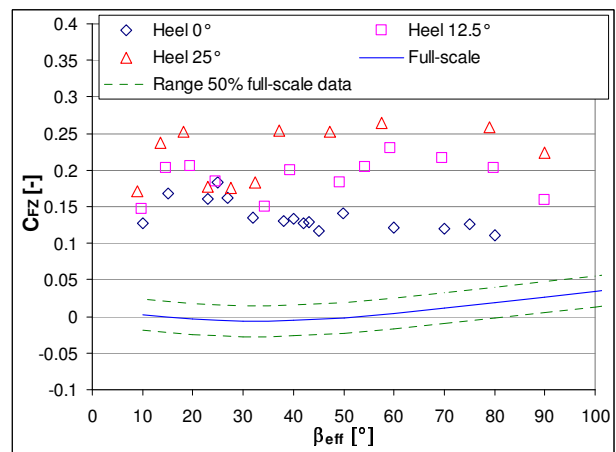


Figure 15. Coefficient of force up the mast for mainsail and genoa III

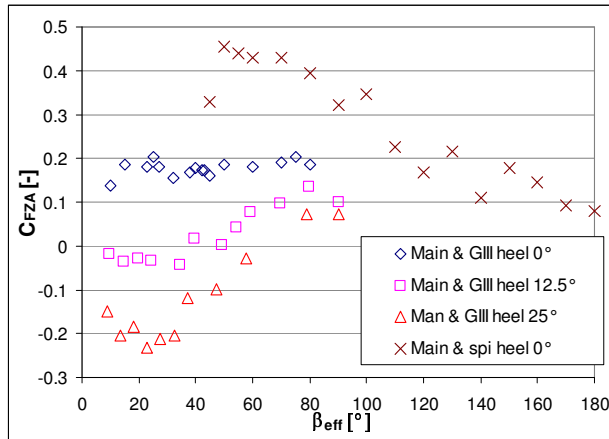


Figure 16. Total vertical force coefficient including hull/deck and rig component

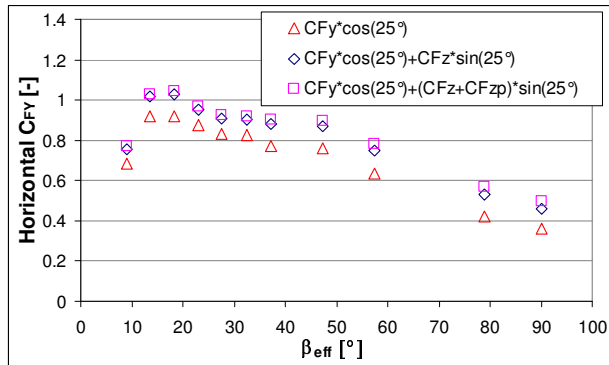


Figure 17. Side force coefficient in horizontal plane at heel 25° for mainsail and genoa III

10. CONCLUSIONS

Both full-scale and wind tunnel testing have difficulties associated with them. In the wind tunnel care must be taken to model the flow correctly and good trimming of the sails is crucial. Full-scale measurements on the other hand are conducted in an unsteady environment and it is difficult to measure all relevant data accurately. As a result the scatter in the full-scale data is significant. It is smaller for tests conducted with mainsail and genoa III compared to measurements made with mainsail and spinnaker.

Nevertheless the wind tunnel and full-scale relate to each other well. The downwind results tend to agree better than the upwind results. In the wind tunnel the sail forces measured include the interaction effect between hull/deck and sails. This effect needs to be isolated to improve the correlation with the full-scale results.

An aerodynamic force acting up the mast is present when a yacht is sailing. It is mainly due to the flow around the hull/deck and the interaction between the hull/deck and the sails. It is significant and should be included in aerodynamic force models. A better understanding of the

origin of this force is required before an improved force model can be developed. Further work using both wind tunnel and full-scale testing is planned to achieve this.

References

1. Herman, J.S., *A Sail Force Dynamometer: Design, Implementation and Data Handling*, in *Dept of Ocean Engineering*. 1988, Massachusetts Institute of Technology: Cambridge.
2. Masuyama, Y. and T. Fukasawa. *Full Scale Measurement of Sail Force and the Validation of Numerical Calculation Method*. in *The 13th Chesapeake Sailing Yacht Symposium*. 1997. Annapolis: SNAME.
3. Hochkirch, K., *Entwicklung einer Meßyacht zur Analyse der Segelleistung im Originalmaßstab (Design and Construction of a Full-Scale Measurement System for the Analysis of Sailing Performance)*, in *Institut für Schiffs- und Meerestechnik*. 2000, Technische Universität Berlin: Berlin.
4. Flay, R.G.J., *A twisted flow wind tunnel for testing yacht sails*. *Journal of Wind Engineering and Industrial Aerodynamics*, 1996. **Vol 63**: p. pp 171-182.
5. Jackson, P.S. *An Improved Upwind Sail Model for VPPs*. in *The 15th Chesapeake Sailing Yacht Symposium*. 2001. Annapolis: SNAME.
6. Locke, N.J., *Lift and Drag Distributions of Sails from Wind Tunnel Wake Surveys*, in *Mechanical Engineering Department*. 1994, University of Auckland: Auckland.
7. Marchaj, C.A., *Aero-Hydrodynamics of Sailing*. 2nd Edition ed. 1988, London: Adlard Coles.
8. Claughton, A. *Developments in the IMS VPP Formulations*. in *The 14th Chesapeake Sailing Yacht Symposium*. 1999. Annapolis: SNAME.
9. Campbell, I.M.C. *Optimisation of a Sailing Rig using Wind Tunnel Data*. in *The 13th Chesapeake Sailing Yacht Symposium*. 1997. Annapolis: SNAME.
10. Flodén, D. and P. Johansson, *Effects of Heel and Twist in Velocity Prediction Programs*, in *Department of Naval Architecture and Ocean Engineering*. 2001, Chalmers University of Technology: Göteborg, Sweden.